Communicating the deadly consequences of global warming for human heat stress

Tom K. R. Matthews[a,1], Robert L. Wilby[b], and Conor Murphy[c]

[a]School of Natural Sciences and Psychology, Liverpool John Moores University, Liverpool L3 3AF, Merseyside, United Kingdom; [b]Department of Geography, Loughborough University, Loughborough LE11 3TU, Leicestershire, United Kingdom; and [c]Irish Climate Analysis and Research Units (ICARUS), Department of Geography, Maynooth University, Kildare, Ireland

Edited by James Hansen, Columbia University, New York, NY, and approved February 21, 2017 (received for review October 25, 2016)

In December of 2015, the international community pledged to limit global warming to below 2 °C above preindustrial (PI) to prevent dangerous climate change. However, to what extent, and for whom, is danger avoided if this ambitious target is realized? We address these questions by scrutinizing heat stress, because the frequency of extremely hot weather is expected to continue to rise in the approach to the 2 °C limit. We use analogs and the extreme South Asian heat of 2015 as a focusing event to help interpret the increasing frequency of deadly heat under specified amounts of global warming. Using a large ensemble of climate models, our results confirm that global mean air temperature is nonlinearly related to heat stress, meaning that the same future warming as realized to date could trigger larger increases in societal impacts than historically experienced. This nonlinearity is higher for heat stress metrics that integrate the effect of rising humidity. We show that, even in a climate held to 2 °C above PI, Karachi (Pakistan) and Kolkata (India) could expect conditions equivalent to their deadly 2015 heatwaves every year. With only 1.5 °C of global warming, twice as many megacities (such as Lagos, Nigeria, and Shanghai, China) could become heat stressed, exposing more than 350 million more people to deadly heat by 2050 under a midrange population growth scenario. The results underscore that, even if the Paris targets are realized, there could still be a significant adaptation imperative for vulnerable urban populations.

climate change | heat stress | megacities | extreme heat | CMIP5

Air temperatures near the surface of Earth are rising. At the time of writing, 2015 was the warmest year globally since observations began (Fig. 1*A*). Higher average air temperatures coincide with more frequent periods of extremely hot weather (1, 2), which in turn, have adverse consequences for human well-being and economic productivity (3–5). The health impacts of rising air temperature are compounded by attendant increases in atmospheric water vapor (6), which reduces humans' ability to dissipate heat (7).

Apparent temperature (8) translates the humidity effect into an index that provides a "feels-like" temperature. Although far from the only metric of its type, it is among the most widely used to communicate episodes of extreme heat (9, 10). For example, the US National Weather Service (NWS) approximates apparent temperature with their heat index (HI) (*Materials and Methods*). The NWS issues warnings when forecasted values persist above 105 °F (with HI = 40.6 °C; hereafter HI40.6)—an operational definition of "dangerous" heat. During 2015, annual maxima for HI were well above average across South Asia and around the Persian Gulf (Fig. 1*B*), with extreme values above 60 °C gaining widespread media attention (11). Some heat-prone megacity regions, such as Karachi (Pakistan) and Kolkata (India), recorded their highest HI values in at least 36 y (Fig. 1 *B*–*D*). The extraordinary heat had deadly consequences, with over 3,400 fatalities reported across India and Pakistan alone (www.emdat.be).

In the context of a warming climate, occurrence of such extreme HI conditions should not be surprising. By definition, the HI has temperature sensitivity much greater than unity at high values (Fig. S1). This nonlinearity is common to temperature–humidity heat stress indicators (12), because for a given relative humidity, latent heat cooling capacity decreases at an accelerating rate in response to the rise in vapor pressure governed by the Clausius–Clapeyron relation. Without counteracting reductions in relative humidity, higher air temperatures drive yet greater increments in HI. This temperature sensitivity is underlined in Fig. 2, which shows HI derived from the model integrations of the Coupled Model Intercomparison Project Phase 5 (CMIP5) (13). Comparing the decade 1979–1988 with 2090–2099, it is evident that extreme HI values (here defined as the 99.9th percentile) over land rise much faster in response to global mean air temperature increase than either mean or extreme air temperatures.

Given the threat already posed by heat stress worldwide (14), such temperature sensitivity is of significant concern. Projections of changes in heat stress have accordingly received attention from the research community (9, 10, 15). For upper-bound, end of 21st century warming, heat in some regions could exceed the physiological tolerance of humans (16), with presently rare heat thresholds being crossed far more regularly (15). The frequency of hot extremes has also been observed to be highly sensitive to global mean temperature increase (2), which is expected to drive increasing heat stress for little additional climate change (17). Even limiting warming to 2 °C since preindustrial (PI) is considered unlikely to avoid an intensification of severe heat events (18).

Mindful of these impacts and sensitivity, we examine the extent to which the global warming limits of 1.5 °C and 2 °C agreed on in Paris by the international community (19) may avoid dangerous climate change from a heat stress perspective. The issue is explored by assessing heat stress projections as a function of global temperature change. This approach has been applied elsewhere in climate impacts research and permits quantification of sensitivity

Significance

Extremely hot weather can have deadly human consequences. As the climate warms, the frequency and intensity of such conditions are expected to increase—among the most certain negative impacts expected under global warming. Concerns about dangerous climate change have encouraged the international community to commit to limiting global temperature changes to below 2 °C above preindustrial. Although lauded as a great achievement to avoid dangerous climate change, we find that, even if such aspirations are realized, large increases in the frequency of deadly heat should be expected, with more than 350 million more megacity inhabitants afflicted by midcentury. Such conclusions underline the critical role for ambitious adaptation alongside these climate change mitigation targets.

Author contributions: T.K.R.M., R.L.W., and C.M. designed research; T.K.R.M. performed research; T.K.R.M. analyzed data; and T.K.R.M., R.L.W., and C.M. wrote the paper.

The authors declare no conflict of interest.

This article is a PNAS Direct Submission.

[1]To whom correspondence should be addressed. Email: t.r.matthews@ljmu.ac.uk.

This article contains supporting information online at www.pnas.org/lookup/suppl/doi:10.1073/pnas.1617526114/-/DCSupplemental.

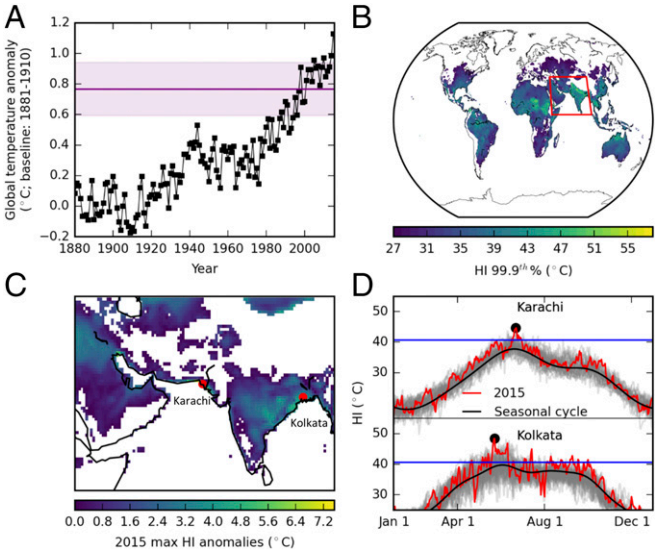

Fig. 1. Mean air temperatures and recent HI extremes. (*A*) Global mean air temperature series defined as the average of the BEST, HadCRUT4, and GISTEMP records. The purple line gives the 1986–2015 mean, with the shaded area representing ±1 SD. (*B*) The 99.9th percentiles of daily HI values, with values <27 °C masked (the lower limit of the HI warning category indicating "caution" to heat stress). (*C*) HI anomaly of 2015 relative to the mean of the annual maximums 1979–2015; negative anomalies are masked as are positive anomalies where absolute HI <27 °C. Note that the domain of *C* is indicated in *B* by the red box. (*D*) Daily mean HI values for the respective regions (1979–2015). Gray curves are individual years 1979–2014; red is 2015.

across a range of policy-relevant warming targets (20–22). We also use temporal and spatial analogs to facilitate communication of these results to the wider public. The use of analogs assumes that conditions already experienced may present similar challenges when manifesting elsewhere or in the future and has been used widely by the climate research community (23). The allure of analogs stems from their potential to educate a wide range of nonspecialists about the complex impacts of climate change, providing a first step to comprehending the unknown (24).

An emphasis on communication is necessary, because warming consistent with the Paris targets has been described as sounding modest enough for the urgency of the situation to be lost on nonexperts (25). Such interpretation may downplay the risk of climate change, which in turn, could make individuals less willing to take action to reduce climate change (26). In reality, the period 1986–2015 was ∼0.8 °C above PI (here defined as 1881–1910) (Fig. 1*A*). Hence, the 1.5 °C and 2 °C Paris targets allow for only another 0.7 °C and 1.2 °C warming [although a global mean temperature rise of 2.7 °C is expected under the current set of intended nationally determined contributions (INDCs)]. In other words, the ambitious targets still commit to between 1.9 and 3.4 times the warming already experienced since the Industrial Revolution, which in turn, propagates into much greater changes in the severity of extreme HI conditions (Fig. 2). Our analysis highlights combined temperature–humidity heat stress impacts as a reason for concern and draws on analogs to illustrate the challenges that may be ahead.

We show the global-scale sensitivity of HI in terms of threshold exceedances (Fig. 3*A*). Sliding 30-y samples of changes in global mean temperature since 1881–1910 from transient CMIP5 simulations are plotted against concurrent changes in bias-corrected global heat stress [defined here as the area-weighted average number of days per year with mean HI ≥ 40.6 °C (nHI40.6)]; the spatial detail behind these projections is illustrated in Fig. S2. The relationship between the global heat stress burden (HSB) and global mean air temperature exhibits nonlinearity that is robust to variants of our method, with higher heat stress sensitivity under increasing temperatures also evident when (*i*) threshold exceedances of 35 °C simplified wet bulb globe temperature (SWBGT) are used [another common heat stress metric (5)] and (*ii*) the transient CMIP5 projections are replaced by pattern-scaled temperature observations and fixed relative humidity (*SI Text*, section 4 and Fig. S3). Notably, the frequency of extreme values increases slower for a reference dry bulb (DB) temperature of 37.6 °C (with equivalent rarity to HI40.6 during the 1979–2005 observational record) as the climate warms. Hence, assessments based on sensitivity of heat extremes' frequency to global temperature change through DB (2) should be regarded as conservative projections of human heat stress.

The spatially-explicit heat stress projections (Fig. S2), highlight that, as global air temperatures rise, the land area experiencing dangerous HI values increases, with poleward expansion particularly evident in the Northern Hemisphere. The frequency of dangerous HI values also increases for those regions that are already impacted. The combined effect of increased area and frequency explains why global heat stress should be expected to follow a nonlinear relationship with global mean air temperature over the range considered here. With the area-weighted mean heat stress defined as $A\bar{N}$ (where A is the fraction of the Earth's land surface experiencing dangerous HI and $\bar{N}$ is the area-weighted mean number of days experienced within this region), nonlinearity will result if both terms are a function of global air temperature (as evident from the product rule of calculus). The practical implication of this relationship is that societies will be disproportionately impacted by heat stress as global temperature increases. Larger populations will be exposed to dangerous HI values, and those people already affected will be subjected to harmful conditions more often and with greater severity.

This nonlinearity also means that any change in global HSB experienced from warming to date will be smaller compared with the same additional warming realized in the future. Such nonlinearity has two implications. First, vulnerable communities may be insufficiently prepared to manage a nonlinear growth in extreme heat risk (27). Second, there could be progressively heavier impacts if the Paris warming targets are missed. According to the median CMIP5 HI curve in Fig. 3*A*, under 1.5 °C global warming, the HSB will be 5.7 times that experienced during the reference period (1979–2005), rising to between ∼12 and 26 times the reference heat stress under 2 °C and 2.7 °C warming, respectively. The avoided impacts of mitigation are shown in Fig. 3*A*, *Inset* by continuing the curves in Fig. 3*A* to 4 °C of global warming. Under

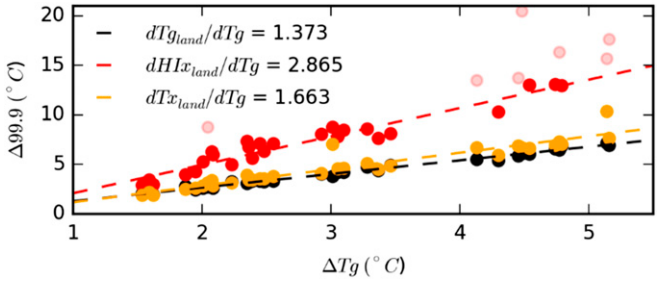

Fig. 2. Relationship between CMIP5 modeled changes in global mean air temperature (ΔTg) and changes in mean air temperature over land (Tg_{land}), extreme temperatures over land (Tx_{land}), and HI values over land (HIx_{land}). Extremes are defined as the 99.9th percentile, and the changes are calculated by differencing the respective values in the last decade of model simulations (2090–2099) relative to the simulated values over the period 1979–1988. Note that we mask HI values >50 °C when computing the regression slope (shown in lighter shading), because this value is the upper limit of the range considered by ref. 8.

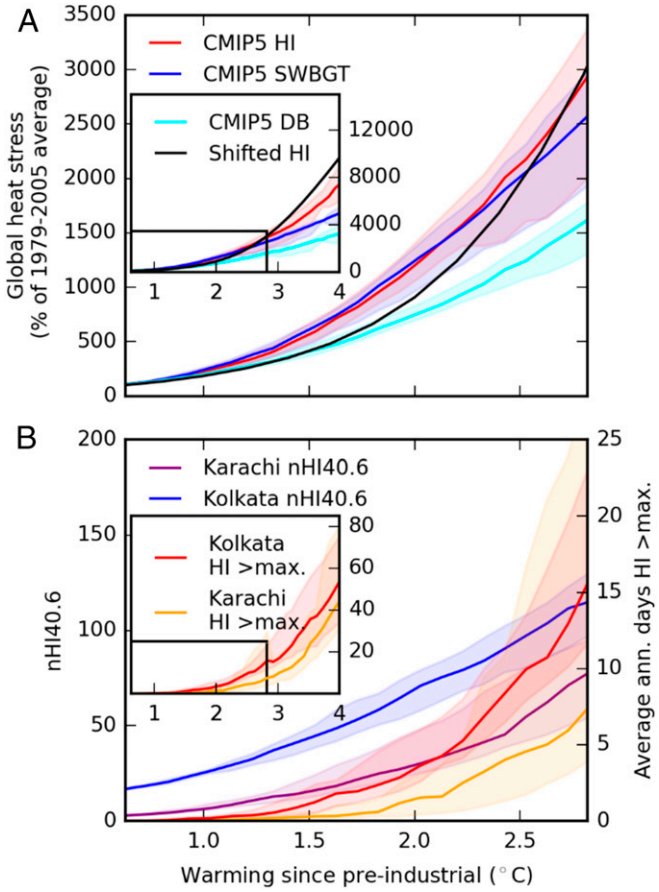

Fig. 3. Global and regional heat stress projected as a function of global warming amounts. (*A*) Global (land) heat stress sensitivity to global air temperature changes, in which lines are medians calculated from the CMIP5 ensemble and the shaded regions span the 25th–75th percentiles. Note that heat stress is defined here as the mean annual number of days exceeding a threshold temperature (40.6 °C, 35 °C, and 37.6 °C for the HI, SWBGT, and DB temperatures, respectively). At this global scale, these metrics are area-averaged. *A*, *Inset* continues the curves to 4 °C warming above PI, with limits in *A* indicated by the black box. (*B*) The same as in *A* but for the named locations, with different units on the *y* axes. Series on *B*, *Inset* axes continues the respective curves from *B* to 4 °C.

these temperatures, HSB as defined by CMIP5 HI reaches more than 75 times the reference value for $A\bar{N}$.

The possible consequences of these projections can be made more tangible by using the recent heatwaves of Karachi and Kolkata as analogs. Because HI40.6 is already expected each year at these locations, likely resulting in some degree of acclimatization (28), we show in Fig. 3*B* counts of annual exceedance of the historical maximum daily mean HI on record alongside HI40.6. The results indicate that HI values in excess of the deadly record set in 2015 would become commonplace in the absence of mitigation efforts (Fig. 3*B*, *Inset*), with more than 40 (50) d per year (a^{-1}) expected in Karachi (Kolkata) under global warming of 4 °C. Although effects are much reduced if warming is limited to levels consistent with the INDCs or the 1.5 °C and 2 °C targets, we highlight that there will likely be significantly increased heat stress, even if mitigation does successfully hold global warming to the ambitious 1.5 °C target. According to the ensemble median, a global warming of 1.5 °C would imply that Kolkata experiences, on average, conditions equivalent to the 2015 record every year; Karachi would experience the same deadly heat about once every 3.6 y. Under 2 °C of global warming, both regions could expect such heat on an annual basis. The potential societal impacts of extreme heat are well-documented (3, 4), and some of these were manifested in Karachi and Kolkata during 2015. Conservative estimates suggest that there were 1,200 heat-related deaths in Karachi and enhanced mortality and economic disruption in Kolkata (29, 30). In this context, the projections of Fig. 3*B* are evidently of significant concern.

We explore the broader potential societal impacts of global warming on heat stress by examining projections for other megacity regions. These locations were identified according to the 21st century population projections from ref. 31, focusing on cities within the top 101 by population size for all three shared socioeconomic pathways (SSPs) (32) and all time slices considered by the authors (2010–2100) (*Materials and Methods*). Our subset of 44 cities accounted for 0.4 billion people in 2010 and is projected to reach between 0.94 and 1.1 billion by 2100 depending on the SSP. For each of these megacities, we identified under which warming scenarios they may begin to experience heat stress annually (using the criteria from the CMIP5 ensemble median projection of nHI40.6 $\geq$ 1) [full information of this city-level assessment, including identification of heat-stressed cities, is in *SI Text*, section 3 (Tables S1–S4)]. We also show in Tables S2–S4 the historical spatial analogs (megacities) that best match the conditions (nHI40.6 and values of the HI 99.9th percentiles) in cities projected to become newly heat stressed.

Fig. 4*A* indicates that, with 1.5 °C of global warming, a number of city regions in West Africa and South and East Asia can expect to experience heat stress for the first time. Lagos (Nigeria), for example, would be newly heat stressed according to our definition and could expect nHI40.6 similar to that endured by Delhi (India) during the reference climate of 1979–2005. The closest historical analog for Shanghai (China)—also newly heat stressed—would be Karachi. Globally, over 40% of these 44 largest cities would be annually heat stressed for a warming of 1.5 °C (Fig. 4*B*), representing a doubling relative to the reference period. With temperatures 2 °C above PI, no additions are made to the list of newly heat-stressed cities, but this absence reflects the spatial distribution of our sampled locations. Under even higher temperature change scenarios, new cities annually experiencing heat stress continue to emerge. For the INDC level of 2.7 °C warming, for example, the largest city in the world at present (Tokyo, Japan) and the Chinese megacity of Beijing could be among those affected. With 4.0 °C warming, nearly 80% of the 44 megacities could be annually heat stressed, including New York and Rio de Janeiro.

Fig. 4*C* suggests that those cities already accustomed to extreme heat can expect larger increases in extreme HI values under the respective warming scenarios (consistent with information in Fig. S1). Use of these city exemplars reinforces the point that, for progressively higher warming amounts, not only will heat stress spread to new populations but those already exposed will be challenged by the largest increases in HI intensity.

The heat stress threat posed by climate change is accentuated by assumed population growth over the coming century. To explore the combined effect of warming and population change in these 44 cities, we defined a population-weighted HSB as the CMIP5 ensemble median nHI40.6 multiplied by the population for each city. By computing the metric using HI projections for different amounts of global warming combined with population projections for a plausible range of years (Fig. 5*A*), we provide insight into the possible effects of specified climates prevailing during particular time periods (Fig. 5*B*). By averaging over all combinations (of years/warming amounts) and SSPs, we can then rank the cities according to their projected HSB over the 21st century (*Materials and Methods* has more details of this procedure; Fig. 5*C*). Note that our method yields insight into conditions beyond the range of specific representative concentration pathways (RCPs) driving the CMIP5 ensemble. For example, the time-evolving impact of stabilizing temperatures at 1.5 °C above PI can be assessed (by simply reading the relevant *x* coordinate in Fig. 5*B*).

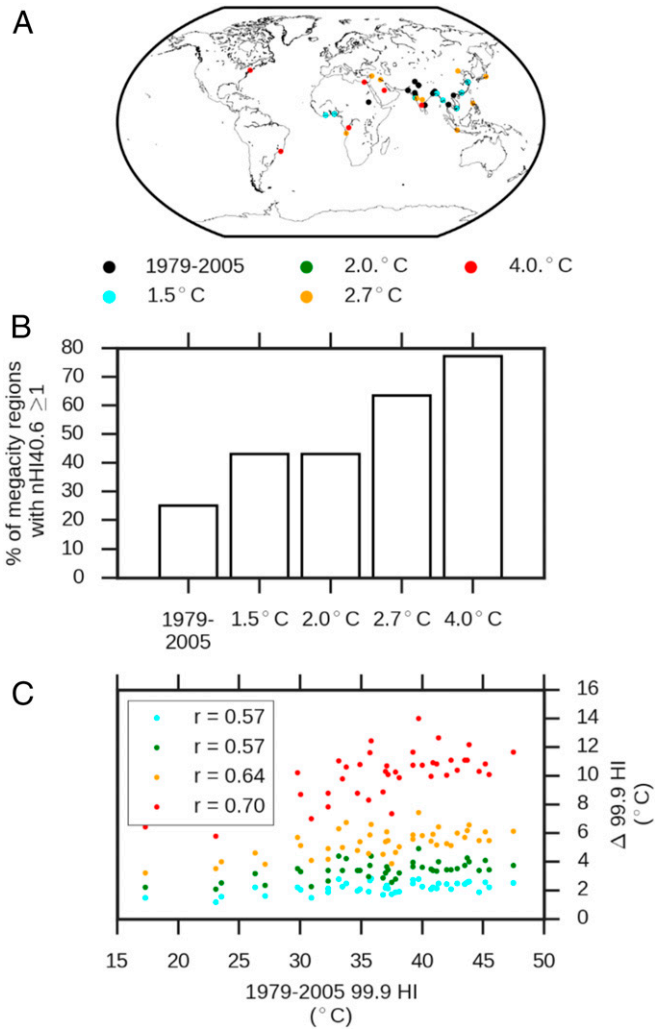

Fig. 4. Changes in heat stress for global city regions under various scenarios of global warming. (*A*) City regions experiencing annual heat stress (nHI40.6 ≥ 1) for the first time under different warming amounts according to the CMIP5 ensemble median. Black circles mark locations already experiencing heat stress during the 1979–2005 reference period. Note that the names of these cities are available in Tables S1–S4. (*B*) CMIP5 ensemble median percentage of megacities experiencing common heat stress under the respective warming amounts. (*C*) Changes in the CMIP5 ensemble median 99.9th HI percentile as a function of the observed 99.9th HI percentile during the 1979–2005 reference period. Values for HI > 50 °C have been masked out of this plot and the correlations in *Inset* (see Fig. 2 legend). These correlations (*r* values) quantify the strength of the positive relationship plotted. Note that the critical *r* value for rejection of the null hypothesis ($r = 0$) is ±0.30 for 42 df at the 0.05 level; hence, all reported values are interpreted as significant.

This analysis suggests that South Asian cities will remain the most heat stressed over the coming century, because 6 of the top 10 by HSB are located in Pakistan, India, or Bangladesh. African cities also feature prominently, with Lagos (Nigeria), Abidjan (Ivory Coast), and Khartoum (Sudan) taking 3 of the remaining 4 spots in the top 10. Notably, Lagos and Abdijan are also projected to realize some of the largest relative changes in HSB (the largest and third largest, respectively; Ho Chi Minh is projected to experience the second largest change), which is because of a combination of rapid population growth and sharp increases in nHI40.6. For example, under 1.5 °C warming, the CMIP5 ensemble median projects that Lagos could see a 106-fold increase in nHI40.6 relative to 1979–2005; under SSP2, population in Lagos peaks during 2070–2099, with an 11-fold increase relative to 1995. A 1.5 °C warmer climate at the end of this century would, therefore, result in an HSB more than 1,000 times greater than the recent past for Lagos. Across all megacities, we estimate that, with this level of warming under SSP2 and as early as the middle of the 21st century, more than 350 million more people (a fourfold increase) could be exposed to heat stress annually compared with the 1979–2005 reference period.

In summary, we emphasize that the potentially deadly consequences of heat stress linked to global warming, even if limited to the 1.5 °C Paris target, should not be overlooked. More of the Earth's land surface could experience dangerous heat, and those regions already exposed could encounter such conditions more often. Although the challenge of reaching a universal definition of dangerous heat is acknowledged—in terms of metric, timing, and duration—the fact remains that conditions that have historically challenged (and overwhelmed) those living in some of the most heat-stressed regions on Earth could become much more frequent. Population growth in vulnerable regions will add to the challenge. We used megacities to quantify the impacts of these combined climate and societal pressures but acknowledge that the spatially coarse climate models used cannot resolve the specific city-scale microclimates (33) in detail. Nonetheless, we consider it unlikely that projections for cities are overly pessimistic given that heat stress amplification associated with global warming is believed to be no less severe in urban environments (34). Indeed, our frequency-based analysis of heat stress likely provides a conservative perspective on projected heat stress. We have also shown that regions characterized by historically higher HI extremes can anticipate larger increases in the HI with global temperature rise, meaning more intense heat stress could also result as the 40.6 °C threshold is exceeded by greater amounts.

The high sensitivity to global temperature rise translates into a further doubling of global heat stress moving from 1.5 °C to 2 °C above PI (5.7 and ∼12 times greater than 1979–2005, respectively), which from a human health perspective, provides a strong incentive for limiting global warming to the lower of these targets. However, with a possible 350 million more people exposed to deadly heat by the middle of the century even if this target is met, our analysis shows the critical role for adaptation alongside mitigation to manage the potential societal impacts. In this aspect, urban centers, including the megacities used here to communicate projected heat stress, are recognized as key focal points for action on mitigating and adapting to climate change (35). Some city authorities are already taking steps to limit the effects of extreme heat. For instance, Ahmadabad (India) recently implemented South Asia's first comprehensive heat action plan, which may soon be expanded across the region (36). Given the dual pressures of climate change and population growth on heat stress identified here, we foresee a need for such plans to be adopted more widely across vulnerable regions.

Materials and Methods

HI and Climate Model Simulations. The NWS HI was calculated using the algorithm in ref. 37. The index was evaluated using daily mean modeled fields from CMIP5 for the period 1979–2099, obtained through the Earth System Grid Federation (an inventory of the runs used is shown in the table in *SI Text*, section 1). Model experiments from 2006 onward reflect the RCPs; results for 1979–2005 were taken from the RCPs' constituent "historical" model runs and identified and spliced using available metadata. HI computation requires values of air temperature and relative humidity. The former was available directly from the CMIP5 archive, whereas relative humidity (*RH*) was derived from specific humidity and surface pressure (P_s):

$$RH = \frac{qP_s}{\varepsilon\, e_0 \exp\left[\frac{L}{R}\left(\frac{1}{T_0}-\frac{1}{T}\right)\right]} \times 100, \quad [1]$$

where q is specific humidity (g/g), ε is the ratio of gas constants for water vapor and dry air (0.622 g_{vapor}/g_{dry_air}), e_0 is 610.8 Pa, L/R is 5,423 K (latent heat of vaporization divided by the gas constant for water vapor), T_0 is

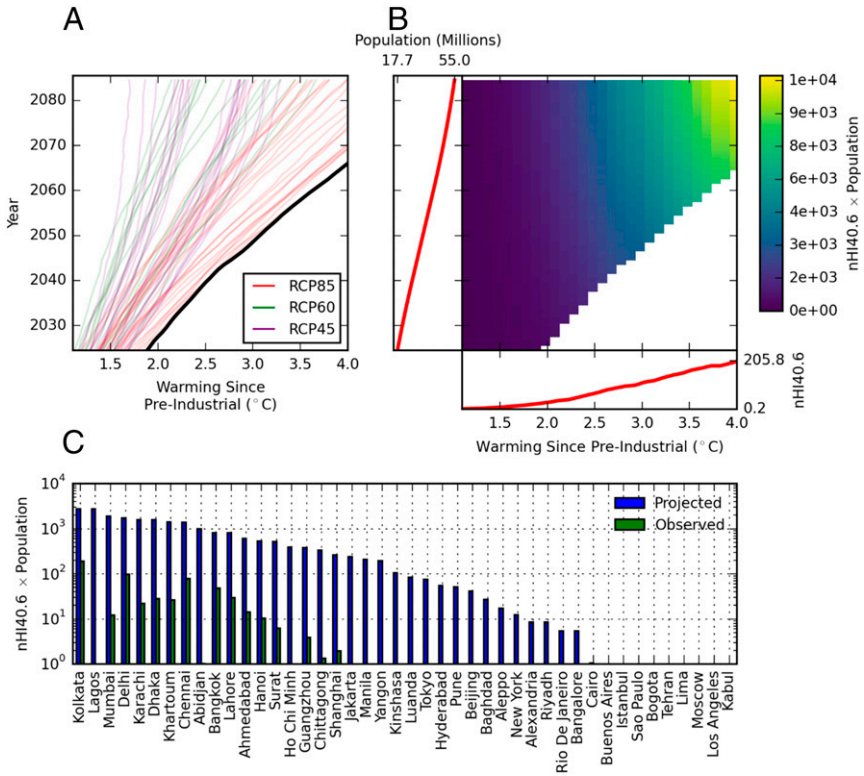

Fig. 5. Population-weighted heat stress throughout the 21st century. (*A*) Running 30-y means of CMIP5 warming since PI. The fastest warming series is plotted with a heavy black line. Warming rates in excess of this are masked in *B*, which shows an example [for Lagos (Nigeria) under SSP2] of the ensemble median HSB for all other combinations of global warming amounts and running 30-y population averages; *Insets* attached to the respective axes show the evolution of the respective variables that are multiplied together to form the matrix. (*C*) The mean HSB projected over the 21st century across all SSP matrices for the respective cities. The reference HSB is computed using HI values for 1979–2005 along with the 1995 population estimate; details of these calculations are in *Materials and Methods*.

273.15 K, and T is the air temperature (Kelvin). P_s is not directly available and was calculated from the hypsometric equation using mean sea-level pressure, air temperature, and surface elevation. These CMIP5 HI values were calculated on native grids for each model before being bilinearly interpolated to the 0.5° × 0.5° observational grid for bias correction and subsequent analysis (details of the observations are given below) (*SI Text*, section 2 has information on the bias corrections).

To explore sensitivity of global heat stress projections to choice of heat stress metric (Fig. 3*A*), the SWBGT was also computed, which required air temperature and vapor pressure. Vapor pressure was obtained from the relative humidity by multiplying Eq. **1** by $e_0 \exp[L/R(1/T_0 - 1/T)/100$.

In Fig. 3*A*, we also showed how the frequency of extreme DB temperatures (a value ≥37.6 °C) responds to global warming in the CMIP5 ensemble. The threshold 37.6 °C was chosen, because we identified that this value had the same nonexceedance probability (99.95%) as an HI value of 40.6 °C in the concurrent observational dataset (see below for details of the observations).

HI and Observations. For observations, the Watch Forcing Data European Reanalysis (ERA) Interim (WFDEI) meteorological dataset (38) (1979–2014) was used. As with the CMIP5 data, HI and SWBGT values were calculated from daily mean air temperature and specific humidity; surface pressure was, however, available directly, eliminating the need for hypsometric adjustment. To place conditions in South Asia during 2015 into context (Fig. 1*C*), observed HI values were bridged to this year using data from the European Centre for Medium Range Weather Forecasting (ECMWF) ERA Interim (39) interpolated to the 0.5° × 0.5° WFDEI grid through a point by point regression. The required linear functions were calibrated on the overlapping 1979–2014 data and forced with ECMWF data in 2015.

For the megacities of Karachi and Kolkata (Fig. 1*D*), HI values from the WFDEI data were similarly extended via regression, but both series (ECMWF and WFDEI) were first interpolated to their respective coordinates (Karachi: 24.86° N, 67.01° E; Kolkata: 22.57° N, 88.36° E). The amount of explained variance (r^2) for these city-specific regressions exceeded 0.95. Note that ERA Interim HI values were calculated analogously for the WFDEI data, with the exception that relative humidity first had to be calculated from dew point air temperature. Full details of how projections were generated for the specific city regions are provided in *SI Text*, sections 2 and 3.

Heat Stress as a Function of Air Temperature Changes. To assess sensitivity of heat stress to global mean air temperature changes, the daily exceedances of HI40.6 computed from each CMIP5 ensemble member at each grid point were first summed annually and then averaged spatially (accounting for grid cell area) to produce series of the global mean number of days above HI40.6. These series were then averaged over running 30-y periods (yielding nHI40.6). Over the same 30-y intervals, temperature changes since PI in the corresponding CMIP5 model runs were calculated by (*i*) calculating the model-simulated difference relative to 1979–2005 and (*ii*) adding the observed warming experienced in 1979–2005 relative to 1881–1910 to this amount. The observed warming in 1979–2005 (0.63 °C) was calculated as the average across the ensemble median of the HadCRUT4 (40), BEST (41), and GISTEMP (42) global mean air temperature series. To prepare Fig. 3, statistics were calculated by linearly interpolating the global mean air temperature (the x values) vs. heat stress (the y values) relationship to a regular spacing of 0.1 °C for each model run and then calculating median and percentile statistics across this interpolated array.

Where the heat stress impacts associated with a given warming scenario are shown (Fig. 4), heat stress conditions were sampled for simulated 30-y climates matching the given global warming amount most closely. We specified that the simulated global mean temperature had to be within an arbitrary tolerance of ±0.075 °C to be considered representative of the specified warming scenario and hence, included in the ensemble statistics.

Population-Weighted Heat Stress. To assess the combined effects of population growth and global warming on city-level heat stress throughout the 21st century, we used projections from ref. 31 available for three SSPs and years 2010, 2025, 2050, 2075, and 2100. We focused on those 44 cities that remained in the top 101 for each of these time slices across three SSPs. Projections for these cities were then linearly interpolated to annual resolution (2010–2099).

We also obtained the 1995 population for each city from ref. 43 to compute the reference HSB over the period 1979–2005. These burdens were calculated by multiplying nHI40.6 for a specified warming amount for each city ($nHI40.6_{City}$) by the respective population (P_{City}). The term $nHI40.6_{City}$ was computed as a function of global warming amounts in 0.1 °C increments analogous to the global-scale metrics (*Materials and Methods, Heat Stress as a Function of Air Temperature Changes*) but without the spatial-averaging step. The ensemble median $nHI40.6_{City}$ was then multiplied by all possible running 30-y population averages for each city, giving insight into the HSB for a wide range of scenarios. We masked combinations of warming amounts (which control $nHI40.6_{City}$) and years that required faster rates of warming than the maximum recorded across the CMIP5 ensemble (Fig. 5*A*). The average 21st century HSB for each SSP was, therefore, calculated from

$$HSB_{City,SSP} = \frac{1}{\sum H(T_g,\ i,\ j)} \sum_i \sum_j \mathrm{nHI40.6}_{City_i} \times P_{City_j} \times H(T_g,\ i,\ j),$$

where the subscripts i and j index the global warming amounts and years, respectively; $H(T_g,\ i,\ j)$ is a Heaviside function that evaluates to one (zero) if the warming amount i is less (more) than the maximum CMIP5 global warming (T_g) for the 30-y period j. Averaging $HSB_{City,SSP}$ across three SSPs yields the 21st century HSB plotted in Fig. 5*C*. Reference HSB was calculated by multiplying the observed (1979–2005) $nHI40.6_{City}$ by the 1995 population.

In the text, we also cite the number of megacity inhabitants with ensemble median nHI40.6 ≥ 1 for a +1.5 °C climate ($n_{1.5}$), which was computed as

$$n_{1.5} = \sum_{City} H(\mathrm{nHI40.6}_{City}, 1.5°\mathrm{C}) \times P_{City,2050},$$

where the Heaviside function evaluates to one (zero) if nHI40.6 for the respective *City* is ≥1. $P_{City,2050}$ denotes the 30-y mean population projection (according to SSP2 for this location and the 30-y period centered on 2050).

Data and Code Availability. The CMIP5 data underpinning our analysis can be downloaded from any of the nodes of the Earth System Grid Federation (e.g., https://esgf-data.dkrz.de/projects/esgf-dkrz/), whereas the observational (WFDEI) dataset is available via ftp from ftp.iiasa.ac.at. The HadCRUT4, GISTEMP, and BEST global air temperature series can be sourced from https://crudata.uea.ac.uk/cru/data/temperature/, https://data.giss.nasa.gov/gistemp/, and berkeleyearth.org/data/, respectively. The SSP megacity population projections were obtained from the authors of ref. 31, and the 1995 population from ref. 43 is available at https://esa.un.org/unpd/wup/CD-ROM/ (file 12). All processed data and computer code used in the analysis are available from the authors on request.

ACKNOWLEDGMENTS. The anonymous reviewers are thanked for their thoughtful feedback. T.K.R.M. thanks Daniel Hoornweg and Michelle Cloak for their help in accessing the city-level population projections; Peter Thorne for useful discussions; and Tim Lane for assistance with data storage. C.M. acknowledges funding from the Irish Environmental Protection Agency, Grant 2014-CCRP-MS.16.

1. Hansen J, Sato M, Ruedy R (2012) Perception of climate change. *Proc Natl Acad Sci USA* 109(37):E2415–E2423.
2. Fischer EM, Knutti R (2015) Anthropogenic contribution to global occurrence of heavy-precipitation and high-temperature extremes. *Nat Clim Chang* 5(6):560–564.
3. Sheridan SC, Allen MJ (2015) Changes in the frequency and intensity of extreme temperature events and human health concerns. *Curr Clim Change Rep* 1(3):155–162.
4. Dunne JP, Stouffer RJ, John JG (2013) Reductions in labour capacity from heat stress under climate warming. *Nat Clim Chang* 3(6):563–566.
5. Willett KM, Sherwood S (2012) Exceedance of heat index thresholds for 15 regions under a warming climate using the wet-bulb globe temperature. *Int J Climatol* 32(2):161–177.
6. Collins M, et al. (2013) Long-term climate change: Projections, commitments and irreversibility. *Climate Change 2013: The Physical Science Basis*, IPCC Working Group I Contribution to AR5, Ed Intergovernmental Panel on Climate Change (IPCC) (Cambridge Univ Press, Cambridge, UK).
7. Sherwood SC, Huber M (2010) An adaptability limit to climate change due to heat stress. *Proc Natl Acad Sci USA* 107(21):9552–9555.
8. Steadman RG (1979) The assessment of sultriness. Part I: A temperature-humidity index based on human physiology and clothing science. *J Appl Meteorol* 18(7):861–873.
9. Fischer EM, Schär C (2010) Consistent geographical patterns of changes in high-impact European heatwaves. *Nat Geosci* 3(6):398–403.
10. Diffenbaugh NS, Pal JS, Giorgi F, Gao X (2007) Heat stress intensification in the Mediterranean climate change hotspot. *Geophys Res Lett* 34(11):L11706.
11. Samenow J (2015) Iran city hits suffocating heat index of 165 degrees, near world record. *The Washington Post*. Available at https://www.washingtonpost.com/news/capital-weather-gang/wp/2015/07/30/iran-city-hits-suffocating-heat-index-of-154-degrees-near-world-record/?utm_term=.762ca3cb7e4b. Accessed August 18, 2016.
12. Fischer EM, Oleson KW, Lawrence DM (2012) Contrasting urban and rural heat stress responses to climate change. *Geophys Res Lett* 39(3):L03705.
13. Taylor KE, Stouffer RJ, Meehl GA (2012) An overview of CMIP5 and the experiment design. *Bull Am Meteorol Soc* 93(4):485–498.
14. Kjellstrom T (2016) Impact of climate conditions on occupational health and related economic losses: A new feature of global and urban health in the context of climate change. *Asia Pac J Public Health* 28(2 Suppl):28S–37S.
15. Zhao Y, Ducharne A, Sultan B, Braconnot P, Vautard R (2015) Estimating heat stress from climate-based indicators: Present-day biases and future spreads in the CMIP5 global climate model ensemble. *Environ Res Lett* 10(8):84013.
16. Pal JS, Eltahir EAB (2015) Future temperature in southwest Asia projected to exceed a threshold for human adaptability. *Nat Clim Chang* 6(2):197–200.
17. Smith JB, et al. (2009) Assessing dangerous climate change through an update of the Intergovernmental Panel on Climate Change (IPCC) "reasons for concern." *Proc Natl Acad Sci USA* 106(11):4133–4137.
18. Diffenbaugh NS, Scherer M (2011) Observational and model evidence of global emergence of permanent, unprecedented heat in the 20(th) and 21(st) centuries. *Clim Change* 107(3-4):615–624.
19. Rogelj J, et al. (2016) Paris Agreement climate proposals need a boost to keep warming well below 2 °C. *Nature* 534(7609):631–639.
20. Hinkel J, et al. (2014) Coastal flood damage and adaptation costs under 21st century sea-level rise. *Proc Natl Acad Sci USA* 111(9):3292–3287.
21. Frieler K, et al. (2012) Limiting global warming to 2 °C is unlikely to save most coral reefs. *Nat Clim Chang* 3(2):165–170.
22. Seneviratne SI, Donat MG, Pitman AJ, Knutti R, Wilby RL (2016) Allowable CO2 emissions based on regional and impact-related climate targets. *Nature* 529(7587):477–483.
23. Ford JD, et al. (2010) Case study and analogue methodologies in climate change vulnerability research. *Wiley Interdiscip Rev Clim Change* 1(3):374–392.
24. Glantz MH (1991) The use of analogies in forecasting ecological and societal responses to global warming. *Environment* 33(5):10–33.
25. Knutti R, Rogelj J, Sedláček J, Fischer EM (2015) A scientific critique of the two-degree climate change target. *Nat Geosci* 9(1):13–18.
26. van der Linden S (2014) The social-psychological determinants of climate change risk perceptions: Towards a comprehensive model. *J Environ Psychol* 41:112–124.
27. Sterman JD (2011) Communicating climate change risks in a skeptical world. *Clim Change* 108(4):811–826.
28. Ballester J, Robine J-M, Herrmann FR, Rodó X (2011) Long-term projections and acclimatization scenarios of temperature-related mortality in Europe. *Nat Commun* 2:358.
29. Express News Service (2015) Kolkata: Heat claims two more, toll reaches 18. *The Indian Express*. Available at indianexpress.com/article/cities/kolkata/kolkata-heat-claims-two-more-toll-reaches-18/. Accessed August 26, 2016.
30. Burke J (2015) India heatwave kills more than 500 people. *The Guardian*. Available at https://www.theguardian.com/world/2015/may/25/india-heatwave-deaths-heatstroke-temperatures. Accessed August 26, 2016.
31. Hoornweg D, Pope K (September 24, 2016) Population predictions for the world's largest cities in the 21st century. *Environ Urban*, 10.1177/0956247816663557.
32. O'Neill BC, et al. (2014) A new scenario framework for climate change research: The concept of shared socioeconomic pathways. *Clim Change* 122(3):387–400.
33. Stone B (2012) *The City and the Coming Climate: Climate Change in the Places We Live* (Cambridge Univ Press, New York).
34. Oleson KW, et al. (2015) Interactions between urbanization, heat stress, and climate change. *Clim Change* 129(3–4):525–541.
35. Reckien D, et al. (2014) Climate change response in Europe: What's the reality? Analysis of adaptation and mitigation plans from 200 urban areas in 11 countries. *Clim Change* 122(1–2):331–340.
36. Knowlton K, et al.; Ahmedabad Heat and Climate Study Group (2014) Development and implementation of South Asia's first heat-health action plan in Ahmedabad (Gujarat, India). *Int J Environ Res Public Health* 11(4):3473–3492.
37. Anderson GB, Bell ML, Peng RD (2013) Methods to calculate the heat index as an exposure metric in environmental health research. *Environ Health Perspect* 121(10):1111–1119.
38. Weedon GP, et al. (2014) The WFDEI meteorological forcing data set: WATCH Forcing Data methodology applied to ERA-Interim reanalysis data. *Water Resour Res* 50(9):7505–7514.
39. Dee DP, et al. (2011) The ERA-Interim reanalysis: Configuration and performance of the data assimilation system. *Q J R Meteorol Soc* 137(656):553–597.
40. Morice CP, Kennedy JJ, Rayner NA, Jones PD (2012) Quantifying uncertainties in global and regional temperature change using an ensemble of observational estimates: The HadCRUT4 data set. *J Geophys Res Atmos* 117(D8):D08101.
41. Rohde R, et al. (2013) A new estimate of the average Earth surface land temperature spanning 1753 to 2011. Geoinfor Geostat: An Overview *An Overv* 1(1):1–7.
42. Hansen J, Ruedy R, Sato M, Lo K (2010) Global surface temperature change. *Rev Geophys* 48(4):RG4004.
43. United Nations, Department of Economic and Social Affairs PD (2014)World Urbanization Prospects: The 2014 Revision, CD-ROM Ed. Available at https://esa.un.org/unpd/wup/CD-ROM/. Accessed March 10, 2017.
44. Rye CJ, Arnold NS, Willis IC, Kohler J (2010) Modeling the surface mass balance of a high Arctic glacier using the ERA-40 reanalysis. *J Geophys Res Earth Surf* 115:F02014.
45. Matthews T, Hodgkins R, Guðmundsson S, Pálsson F, Björnsson H (2015) Inter-decadal variability in potential glacier surface melt energy at Vestari Hagafellsjökull (Langjökull, Iceland) and the role of synoptic circulation. *Int J Climatol* 35(10):3041–3057.